scientific reports

Check for updates

OPEN

Virgin and photo-degraded microplastics induce the activation of human vascular smooth muscle cells

Elisa Persiani[1], Antonella Cecchettini[1,2], Sofia Amato[1], Elisa Ceccherini[1], Ilaria Gisone[1], Agnese Sgalippa[1], Chiara Ippolito[2], Valter Castelvetro[3], Tommaso Lomonaco[3] & Federico Vozzi[1]✉

Microplastics (MPs) are an emerging environmental issue due to their accumulation in ecosystems and living organisms. Increasing evidence shows that MPs impact vascular function, with recent studies finding MPs in atheromas linked to cardiovascular events. Since vascular smooth muscle cells (VSMCs) are crucial to maintaining vascular function, this study examined how MPs activate VSMCs, leading to cardiovascular diseases like atherosclerosis and vascular calcification. The study used polyethylene (PE) and polystyrene (PS), common in food packaging, as "virgin" or photo-degraded to simulate environmental conditions. VSMC viability, apoptosis, cytotoxicity, inflammation, and activation markers were evaluated. PE and PS affected VSMC viability, induced apoptosis, and triggered pathological changes such as altered migration and proliferation. Key markers like RUNX-2 and galectin-3, which regulate cardiovascular pathology, were activated, alongside the inflammasome complex. In conclusion, MPs can induce harmful activation of VSMCs, posing potential health risks through inflammation, cell damage, and phenotypic changes. Understanding these toxic mechanisms may reveal critical pathways for intervention and prevention.

Keywords Microplastics, Vascular smooth muscle cells, Phenotypic switch, Polyethylene, Polystyrene

Abbreviations

BMF	Bcl-2 Modifying Factor
HCASMCs	Human Coronary Artery Smooth Muscle Cells
LDH	Lactate Dehydrogenase
MNPs	Micro/nano plastics
MP(s)	Microplastic(s)
NPs	Nanoplastics
PE	Polyethylene
PS	Polystyrene
RUNX-2	Runt-related transcription factor 2
VSMCs	Vascular Smooth Muscle Cells
α-SMA	α-smooth muscle actin

Microplastics (MPs) are ubiquitous pollutants that can take hundreds to thousands of years to decompose, and consequently, their management is becoming an increasingly pressing issue. Ingestion, inhalation, and dermal contact are possible routes of MP exposure that pose threats to human health[1–3]. MPs can, therefore, enter the human body through the respiratory tract, digestive system, or blood circulation and then travel to different organs and tissues[1,3,4]. Despite numerous efforts, little is known about the MPs' influence on the human cardiovascular system. Several studies have described plastic fragment bioaccumulation in cardiac tissue. Recent evidence described the presence of various types of MPs in the human heart and its surrounding tissues of patients undergoing cardiac surgery[5]. Acute exposure to PS-NPs led to the deposition of plastic particles in the hearts of pregnant rats and foetuses[6]. PS-MPs were observed in rat cardiomyocytes directly, exhibiting

[1]CNR Institute of Clinical Physiology, Pisa, Italy. [2]Department of Clinical and Experimental Medicine, University of Pisa, Pisa, Italy. [3]Department of Chemistry and Industrial Chemistry, University of Pisa, Pisa, Italy. ✉email: federico.vozzi@cnr.it

elevated markers of myocardial damage, widespread oxidative stress-induced apoptosis, and a shift toward cardiac fibrosis[7]. PS particles were experimentally used to induce pulmonary embolism, and circulating MPs seem to trigger an inflammatory state, vascular occlusions, and hypercoagulability, at least in a rat model[8]. The hypercoagulable state is directly linked to the development of venous and arterial thrombosis. As a further pro-thrombogenic factor, MPs activated red blood cell aggregation and adhesion to vascular endothelial cells in an in vitro human model[9]. According to Wu et al.[10], MPs have been discovered in human thrombi, which may indicate that MPs have a causal role in cardiovascular diseases. Furthermore, early data on mammals demonstrated that exposure to nanoparticles had a deleterious effect on cardiac electrophysiological function, resulting in lower mitochondrial membrane potentials and early contraction forces[11]. MPs and nanoplastics have recently been found in ex vivo specimens from patients undergoing carotid endarterectomy in the presence of asymptomatic carotid artery disease[12]. Vascular smooth muscle cells (VSMCs) are the most abundant cells in vessels and retain a high plasticity rate[13]. The vast majority of VSMCs within the vessel wall have contractile phenotype, allowing them to maintain vascular functionality. It is characterised by abundant expression of contractile proteins, such as α-smooth muscle actin, or α-SMA, and negligible proliferation[13–15]. In response to stressor agents or endothelial and vessel injury, contractile VSMCs can switch to a synthetic phenotype with acquired proliferative, migratory, and synthetic capabilities, possibly for tissue reparation. The phenotypic transition includes specific marker expression changes, one amongst others is the decrease of α-SMA[14,16]. VSMCs isolated from arteries and cultured in a standard medium containing FBS (generally at 10%) have the ability to migrate and proliferate, acquiring a synthetic, activated phenotype, but they can also survive in the absence of FBS. In this condition, they stop proliferating and migrating and differentiate into a contractile phenotype[17,18].

VSMC phenotypic switching and activation can result in various cardiovascular diseases and dysfunctions, including atherosclerosis and vascular calcification. The transition of VSMC to a pathological phenotype is characterised by an increased expression of molecular biomarkers, such as runt-related transcription factor 2 (RUNX-2) and galectin-3. In particular, RUNX-2 is a key mediator between oxidative stress and vascular calcification[19,20]. Upregulation of RUNX-2 in VSMCs increases the expression of inflammatory cytokines that promote macrophage infiltration and the differentiation of vascular osteoclasts, leading to VSMC osteogenic differentiation and calcification. Furthermore, galectin-3 has been demonstrated to promote a chronic inflammatory state at the cardiovascular level, expressed by inflammatory cells in unstable atherosclerotic plaques[21], and it is necessary for the acquisition of a complete osteoblast-like phenotype, favouring calcification in atherosclerotic plaques[22,23]. Considering that vascular perturbations may drive the phenotypic transition of VSMCs and that MPs have been depicted as cardiovascular stressors, investigating the potential for MPs' role in cardiovascular toxicity in a human model may have enormous social and economic benefits. Polyethylene (PE) and polystyrene (PS) are undoubtedly the top leaders in plastic types used in the food industry for food packaging. However, their massive use as containers has recently raised increasing concerns about the environmental impacts of packaging because of their capacity to disintegrate into MPs[24]. Besides, PE- and PS-MPs may potentially be released by plastic containers and directly ingested, as observed with water bottles[25]. In addition, it is known that plastic debris in the environment undertakes chemical and physical degradation, leading to mechanical as well as molecular fragmentation, resulting in the formation of degradation products, which can then be released, further potentiating the toxic potential[26].

The present study aimed to explore: (1) the potential for virgin and artificially degraded PE and PS particles to affect vascular cell survival and induce cytotoxicity, (2) whether PE- and PS-MPs enhance the expression of the phenotypic switching markers of VSMC, supported by phenotypic changes and, (3) whether the transition is accompanied by the activation of the inflammasome complex, depicting an abnormal, pathological scenario caused by MPs exposure.

Methods

Physiochemical features of microplastics

Virgin materials were composed of cryogenically micronised powders of polyethylene (PE) (density of 0.917 g/cm^3 with an average particle size of 632 µm) and polystyrene (PS) (nominal density of 1.054 g/cm^3 and an average particle size of 564 µm) were kindly gifted by Poliplast S.p.A. (Casnigo, Italy). In particular, the particles exhibited a nominal distribution range from 30 to 1500 µm, with over 10% by volume (or more than 50% by number) below 200 µm. The particles added to cell cultures were typically in the lower range of this distribution, centred around 150 µm, as introduced by pipetting from vigorously stirred aqueous suspensions. The particle sizes allowed for the analysis of consequences related to the contact MP-cells. To accelerate MP photo-oxidative degradation, thus reproducing the environmental conditions, these microplastics were artificially aged for 4 weeks following the procedures described elsewhere[4,27]. Virgin (i.e., unprocessed) MPs were referred to as "0w", whilst artificially aged-photodegraded MPs were defined as "4w". Plastic particle aliquots were stored at -20 °C in amber glass vials until their use. Upon first use, MPs were allowed to equilibrate at room temperature and sterilised through UV light exposure for three consecutive cycles of 15 min under a laminar flow biosafety hood. Regarding the chemical characterisation of the materials used in the present study, please refer to the previously reported[28]. MPs stock at 10 mg/ml were prepared under sterile conditions by diluting each material with PBS and stored at +4 °C. Working suspensions were freshly prepared in cell culture medium (Human Vascular Smooth Muscle Cells Basal medium, Thermo Fisher, Waltham, MA, USA) at 1 mg/mL concentration. This was considered an environmental exposure concentration, as suggested elsewhere[29].

Cell culture

Human Coronary Artery Smooth Muscle Cells (HCASMCs) were purchased from Thermo Fisher (Thermo Fisher, Waltham, MA, USA) and maintained in 25 cm^3 flasks with Human Vascular Smooth Muscle Cells Basal medium (Thermo Fisher, Waltham, MA, USA) added with Smooth Muscle Growth Supplement (Thermo Fisher,

Waltham, MA, USA) and antibiotic-antimycotic solution, at 37 °C in a humidified atmosphere containing 5% CO_2. When experiments started, cells were cultured in Human Vascular Smooth Muscle Cells Basal medium (Thermo Fisher, Waltham, MA, USA) without the addition of serum to evidence the effect on HCASMCs activation imputable only to the MPs treatment and not to the FBS. The medium was changed daily, and trypsinised cells were passaged when reaching a confluence of 90%. Only cell passages from 2 to 5 were used. Before each experiment started, cells were transferred into 96- or 12-multiwell cell culture plates, depending on the assay setting up at a concentration of 7000 cells per cm^2. Cells were allowed to settle in the plates for 24 h, and then MPs were added. Cells were harvested after 72 h of incubation with plastic particles.

Cell viability assessment

The proliferation capacity of HCASMCs was measured through the CellTiter-Blue® Cell Viability Assay kit Promega, Madison, WI, USA). The kit relies on the metabolic potential for viable and healthy cells to reduce resazurin to resorufin, which generates a fluorescence signal proportional to the number of proliferating cells. Following a 72-hour incubation with MPs, HCASMCs were analysed by adding CellTiter-Blue® Reagent (20 µL for each 100 µL cell medium) in a 96-multiwell. Plates were incubated for 2.5 h at 37 °C in a humidified incubator, and fluorescence was measured using a spectrofluorometer (560Ex/590Em) (Fluostar Omega, BMG Labtech, Ortenberg, Germany). A preliminary analysis was conducted to verify that the MPs do not interfere with the results of the plate reader measurements (data not shown).

Cytotoxicity assay

The cytotoxic potential of MPs in HCASMCs was determined with the Cytotoxicity Detection Kit (Merck, Darmstadt, Germany), following the manufacturer's protocol. In summary, after 72 h of HCASMC exposure to MPs, 50 µL of each supernatant was transferred into a new 96-multiwell plate, assayed in duplicates. 50 µL of reaction mixture (prepared by mixing the catalyst and dye solution) were added and allowed to incubate for 30 min at room temperature, protected from light. The absorbance of the samples was measured with a plate reader using a 492 nm wavelength filter. A preliminary analysis was carried out to ensure that the MPs have no impact on the absorbance measurements (data not shown).

Scratch-wound migration assay

HCASMCs were seeded in 12-multiwell culture plates and allowed to grow until confluent in Human Vascular Smooth Muscle Cells Basal medium added with Smooth Muscle Growth Supplement. The confluent cells were wounded by scraping with a sterile 20 µl-pipette tip. At this point, the culture medium was replaced with 1 mg/ml of MPs dispersed in the Human Vascular Smooth Muscle Cells Basal medium only and cultured for 72 h. The rate of wound closure was then monitored at the end of the experiment using images captured with a brightfield microscope (Nikon Eclipse Ts2, Nikon, Tokyo, Japan) at 4× magnification. The digital photographs were visualised and analysed with ImageJ software (National Institutes of Health, Rockville, MD, USA; http://imagej.net/ImageJ). Gap closure for each sample was evaluated as the percentage of area occupied by the gap over the total area of the picture. At least 3 measures were taken for each digital image, and each experiment was run in triplicate.

Immunofluorescence analysis

Samples under investigation were processed for observation and analysis through laser scanning confocal microscopy (LSCM). A 2% paraformaldehyde solution in phosphate buffer (PBS) was used for 15 min to fix cells. Only PBS without calcium and magnesium (Merck, Darmstadt, Germany) was used hereafter. Note that three consecutive washes in PBS were always performed between each of the described steps. Incubations were performed at room temperature unless otherwise stated. Afterwards, the permeabilisation process was conducted by treatment with Triton-X 0,1% in PBS (Merck, Darmstadt, Germany) for 5 min followed by blocking with 5%, BSA (Merck, Darmstadt, Germany), 0,1% Tween-20 (Merck, Darmstadt, Germany) in PBS for 1 h. Subsequently, the cells were incubated overnight at +4 °C with the following primary antibodies: Rabbit MAb Alpha Smooth Muscle Actin (Thermo Fisher, Waltham, MA, USA) 1:200 in blocking solution, Mouse MAb Galectin 3 (Thermo Fisher, Waltham, MA, USA) 1:100 in blocking solution. Goat anti-Mouse Alexa Fluor Plus 488 (Thermo Fisher, Waltham, MA, USA) 1:2000 in blocking solution or Goat anti-Rabbit Alexa Fluor Plus 594 (Thermo Fisher, Waltham, MA, USA) 1:2000 in blocking solution were used as secondary antibodies and samples were incubated for 2 h protected from light. Coverslips were mounted on glass slides using Fluoroshield™ with DAPI (Merck, Darmstadt, Germany). Samples under investigation were processed for observation and image acquisition through a laser scanning confocal microscopy (LSCM) system. All images were captured through a Leica TCS SP8 (Leica Microsystems, Mannheim, Germany) to visualise the samples using an XYZ scan mode and the HC PL APO CS2 40x/1.30 oil objective. Representative confocal images were obtained by 3D function at a resolution of 2048 × 2048 pixels. ImageJ software determined marker fluorescence intensity (1.53o; National Institute of Health, Bethesda, MD, USA). The software was used to quantify α-SMA and galectin-3 expression to find the mean grey value for each image.

RNA extraction and quality evaluation, reverse-transcription

Cell pellets were collected from MPs-exposed samples by vigorous scraping with pipette tips in PSB for subsequent gene expression analysis. Total RNA was extracted using PureLink™ RNA Mini Kit (Thermo Fisher, Waltham, MA, USA) following the manufacturer's instructions. On-column DNase treatment was also performed to improve the efficiency and purity of the starting material. The RNA concentration and purity were determined by spectrophotometry (NanoDrop™ Lite Spectrophotometer, Thermo Fisher, Waltham, MA, USA), and the samples were stored at − 80 °C until use. Complementary DNA (cDNA) was generated from

isolated total RNA (250 ng) using SuperScript™ IV First-Strand Synthesis System (Thermo Fisher, Waltham, MA, USA), following the manufacturer's protocol. No-reverse transcriptase (NRT) controls were also included in the reaction. Samples were stored at -20 °C if not used immediately.

Real-time qPCR analysis

According to the manufacturer's instructions, gene expression analysis was performed with SYBR™ Green-based assay (Thermo Fisher, Waltham, MA, USA). Forward and reverse primers were designed using Primer-BLAST (http://www.ncbi.nlm.nih.gov/tools/primer-blast). All primer pairs were then purchased from Sigma-Aldrich, and a list is provided in Table 1.

GAPDH was used as a housekeeping gene. cDNA obtained from each sample was diluted in DEPC-treated water to a final concentration of 25 ng/µl per well and loaded as triplicates in a reaction plate. No-template controls (NTC) and NRT were included as controls for potential contamination. Real-time PCR amplification and analysis were conducted in a Bio-Rad CFX96™ Real-Time System (Bio-Rad Laboratories Inc., Hercules, CA, USA). PCR amplification was performed using two-step cycling conditions of 95 °C for 3 min, followed by 40 cycles of 95 °C for 10 s and 58 °C for 30 s. After amplification, melting curve analysis was performed by heating to 95 °C for 5 s, then lowering the temperature to 65 °C for 5 s, followed by an increase of 95 °C, while collecting the fluorescent signal to confirm the presence of only a pure, single amplicon.

For post-qPCR analysis, normalisation was done with GAPDH, and relative quantification was obtained using the $2-\Delta\Delta Ct$ algorithm.

Caspase-1 Detection in cell culture medium

To evaluate the potential for MPs to activate a pro-inflammatory status, caspase-1 was measured in HCASMCs culture media after 72 h of treatment with MPs. To this extent, the Caspase-Glo® 1 Inflammasome Assay kit (Promega, Madison, 17 WI, USA) was employed according to the manufacturer's directions. Before each use, all reconstituted reagents of the kit were allowed to equilibrate at room temperature. An aliquot of 20 µL of cell medium from each 96-multiwell plate was transferred to a 96-white multiwell plate. Then, 50 µL/well of Caspase-Glo® 1 Reagent were added to each well for the detection of Caspase-1 or 50 µL/well of Caspase-Glo® 1 YVAD-CHO Reagent to exclude any nonspecific signal generated. Such prepared mixtures were incubated for 1 h at room temperature and protected from light. Relative luminescence units (RLU) were measured using a plate reader.

Statistical analysis

Each test was normalised for the number of cells present in the sample. This number was generated through a standard curve, as described in[4,30]. Briefly, a defined number of HCASMCs was serially diluted and plated, then they were allowed to settle for 24 h, and cell viability was measured as previously described. This created a standard curve, linking the fluorescent value with the number of cells.

One- or two-way ANOVA tests were used as indicated, followed by Fisher's LSD or Dunnett's multiple comparison tests as appropriate, comparing tested samples with the control-untreated HCASMCs (CTRL). All data are presented as the mean ± standard deviation (SD), and a $p < 0.05$ was considered significant. All data were analysed using GraphPad Prism version 9 (GraphPad Software, Boston, Massachusetts USA, www.graphpad.com).

Results

Cell viability decreases and apoptosis increments in HCASMCs upon PE and PS exposure

Cells were cultured in the presence of PE and PS in a serum-free medium to investigate the ability of MP to activate VSMCs. Upon a 72-hour incubation with MPs, HCASMCs were tested for cell viability endpoint assay,

Gene	Primer sequence (5'-3')
GAPDH	FWD: ACATCGCTCAGACACCATGG
	REV: GACGGTGCCATGGAATTTGC
RUNX2	FWD: GATTCTTAACCAACCAGCCTTACC
	REV: AGTGATGTCATTCTGCTCCTCTAA
α-SMA	FWD: AGAGTTACGAGTTGCCTGATG
	REV: GATGAAGGATGGCTGGAACA
Galectin-3	FWD: GCCACTGATTGTGCCTTATT
	REV: CCGTGCCCAGAATTGTTAT
p53	FWD: TGGCCATCTACAAGCAGTCA
	REV: GGTACAGTCAGAGCCAACCT
BMF	FWD: CTATCGGCTTCCTCTCCCTG
	REV: CCCCGTTCCTGTTCTCTTCT

Table 1. Primer pairs list, with forward (FWD) and reverse (REV) sequences. GAPDH: glyceraldehyde-3-phosphate dehydrogenase; RUNX2: runt-related transcription factor 2; α-SMA: smooth muscle actin α; BMF: BH3-only protein.

relying on the metabolic capacity of cells to reduce resazurin at the end of the exposure period (Fig. 1a). When MPs-exposed groups were compared to CTRL, a statistically significant decrease in cell viability was observed for all materials. The differences were comparable for virgin and aged PE particles (1.5-fold decrease for both), whilst PS had a different impact on the reduction of cell viability (1.4 for virgin and nearly 2.0-fold for the aged one). Furthermore, apoptosis was assessed after 72 h of MP exposure using real-time qPCR. As illustrated in Fig. 1b and c, p53 and Bcl-2 Modifying Factor (BMF) showed significant upregulation, with p53 increasing by 1.6 for virgin PS ($p \geq 0.05$) to 3-fold and BMF by 6 to 11-fold.

Cytotoxic potential of virgin and aged PE and PS

To determine the cytotoxic ability of the MP types under analysis, lactate dehydrogenase (LDH) activity released from damaged cells was quantified using a commercially available kit. A general increase in LDH release was observed in all HCASMCs treated samples, which was statistically significant, except for the virgin PE group (Fig. 2). These findings suggest that MPs can trigger plasma membrane damage in the cell population under investigation. The different results found in the unprocessed PE group might indicate a different degree of cell damage, which the presence of LDH or a distinct toxic effect cannot explain.

Migration propensity increases in HCASMCs with PE and PS

The wound healing assay (Fig. 3) demonstrated that HCASMCs cultured with either PE or PS showed an increased migration ability compared to the control group. Indeed, quantification of the area of the gap expressed

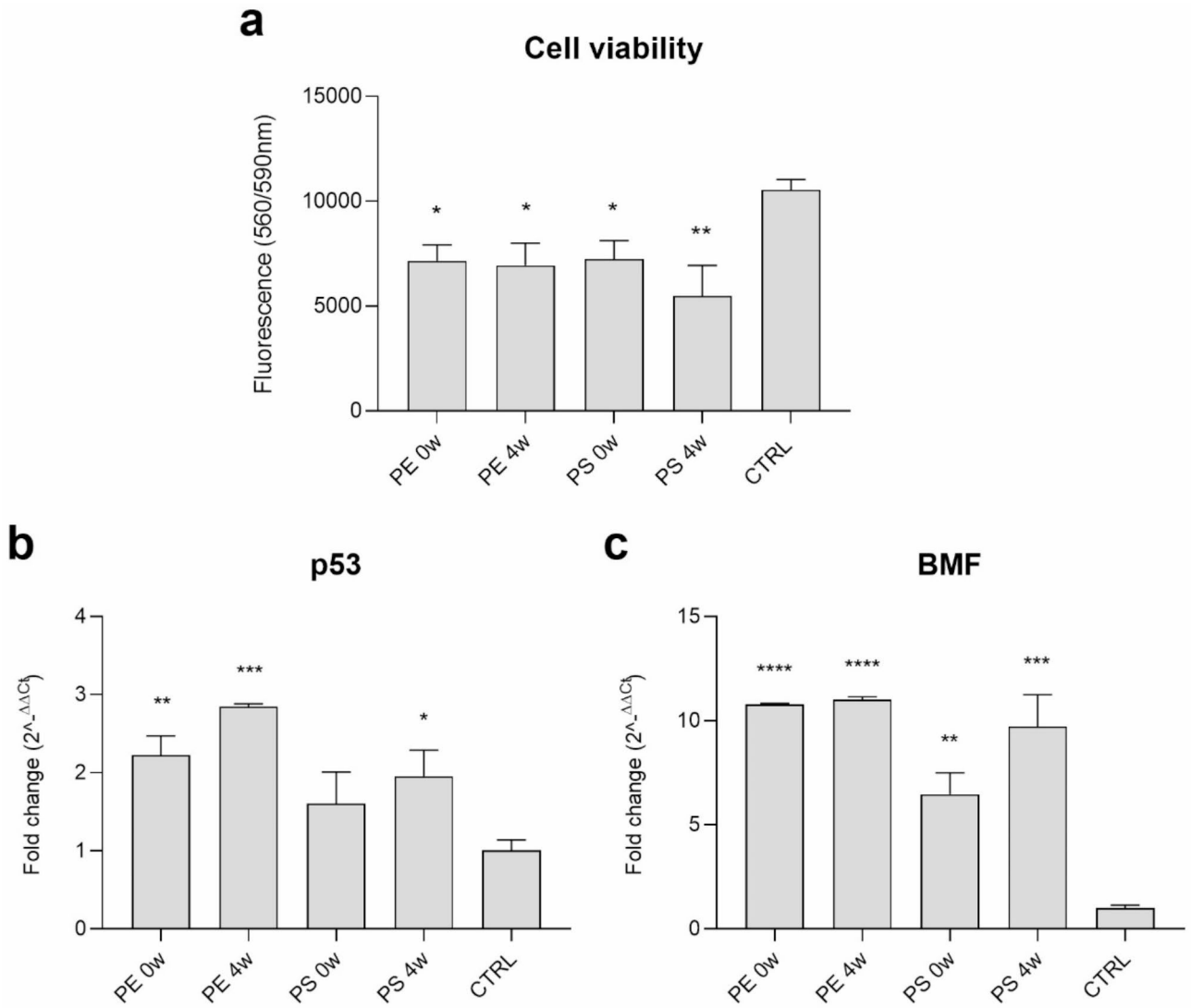

Fig. 1. Comparison of cell health in HCASMCs treated with different types of MPs and controls. In a, cell viability assay and gene expression analysis of p53 b, and BMF in c. Data are presented as the means ± SD. Statistical analysis performed using one-way ANOVA followed by Fisher's LSD post-hoc test. * $p < 0.05$, ** $p < 0.01$, *** $p < 0.001$, **** $p < 0.0001$ compared to CTRL samples. PE: polyethylene; PS: polystyrene. 0w: virgin MP; 4 w: aged-photodegraded MP.

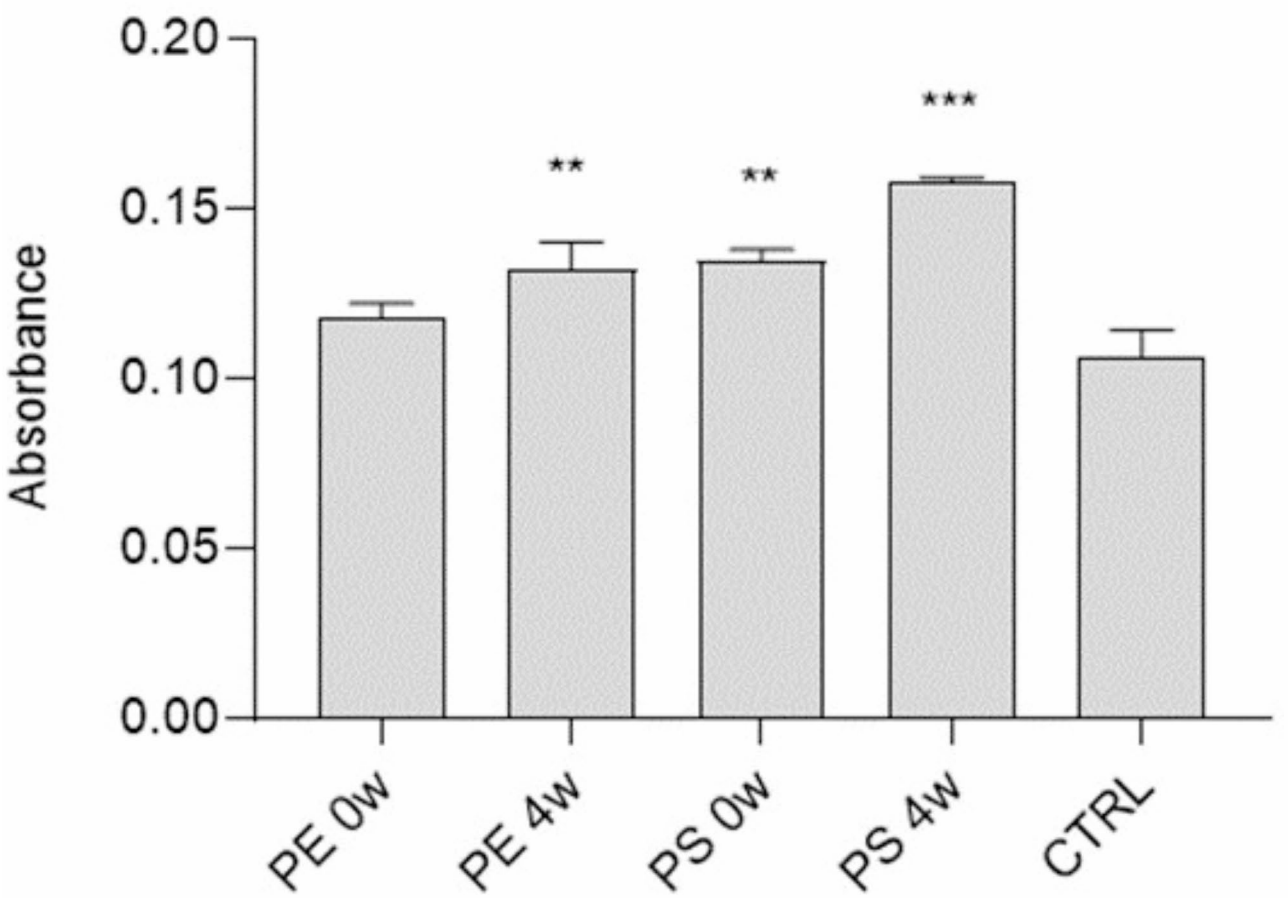

Fig. 2. Measurement of the cytotoxic potential of PE (polyethylene) and PS (polystyrene) 0w (virgin materials) and 4w (aged materials), through quantification of LDH in cell culture media. Data presented as the means ± SD. Statistical analysis performed using one-way ANOVA followed by Fisher's LSD post hoc test. ** $p < 0.01$, *** $p < 0.001$ compared to CTRL.

as a percentage relative to control samples unveiled that the presence of MPs might remarkably increase the migratory ability in HCASMCs (Fig. 3b). The wound healing area substantially disappeared in all treated groups, with similar results between plastic types and photodegradation rates.

HCASMCs phenotype switch induced by PE and PS treatment

The potential for PE and PS to induce the phenotype switching in HCASMCs was explored through immunofluorescence analysis after a 72-hour exposure. Fixed cells were then stained with anti-α-SMA (α–smooth muscle actin) and anti-galectin-3 antibodies. Acquired images of contractile/synthetic type markers expression and cellular morphology were analysed (Fig. 4a). As expected, a high α-SMA signal in cells cultured in the absence of serum was detected, with a reduction in all other analysed samples (Fig. 4b). Galectin-3, instead, showed a markedly increased expression for all the MPs tested compared to the control, excluding for PE 4 W (Fig. 4c). These results were consistent in HCASMCs exposed to MPs, with a lower expression of contractile markers, particularly α-SMA. Real-time PCR confirmed that α-SMA expression was lower in MPs-treated groups (Fig. 4d). However, this was not the case for the aged PS group, where α-SMA was similar to the control group. Galectin-3, as a representative marker for the synthetic, activated form of VSMCs, showed a decrease in signal intensity for CTRL, whilst all MPs-exposed groups showed statistically significant upregulation (Fig. 4e). Treated samples equally expressed RUNX-2 as a marker for synthetic-osteoblastic phenotype, which displayed an upregulation in all samples under analysis compared to CTRL (Fig. 4f). The comparison of immunofluorescence analysis and Real-time PCR results showed substantial accordance in trend for the different MPs. The single channel images for α-SMA and galectin-3 are presented in Supplementary materials for immunofluorescence analysis.

PE and PS activate the inflammasome complex

To explore the ability of PE and PS to induce an inflammatory response in HCASMCs, we examined the presence of caspase-1, an essential component of the inflammasome, using a bioluminescence assay. As reported in Fig. 5, HCASMCs treated with both virgin and aged PE- and PS-MPs exhibited a significant up-regulation of caspase-1

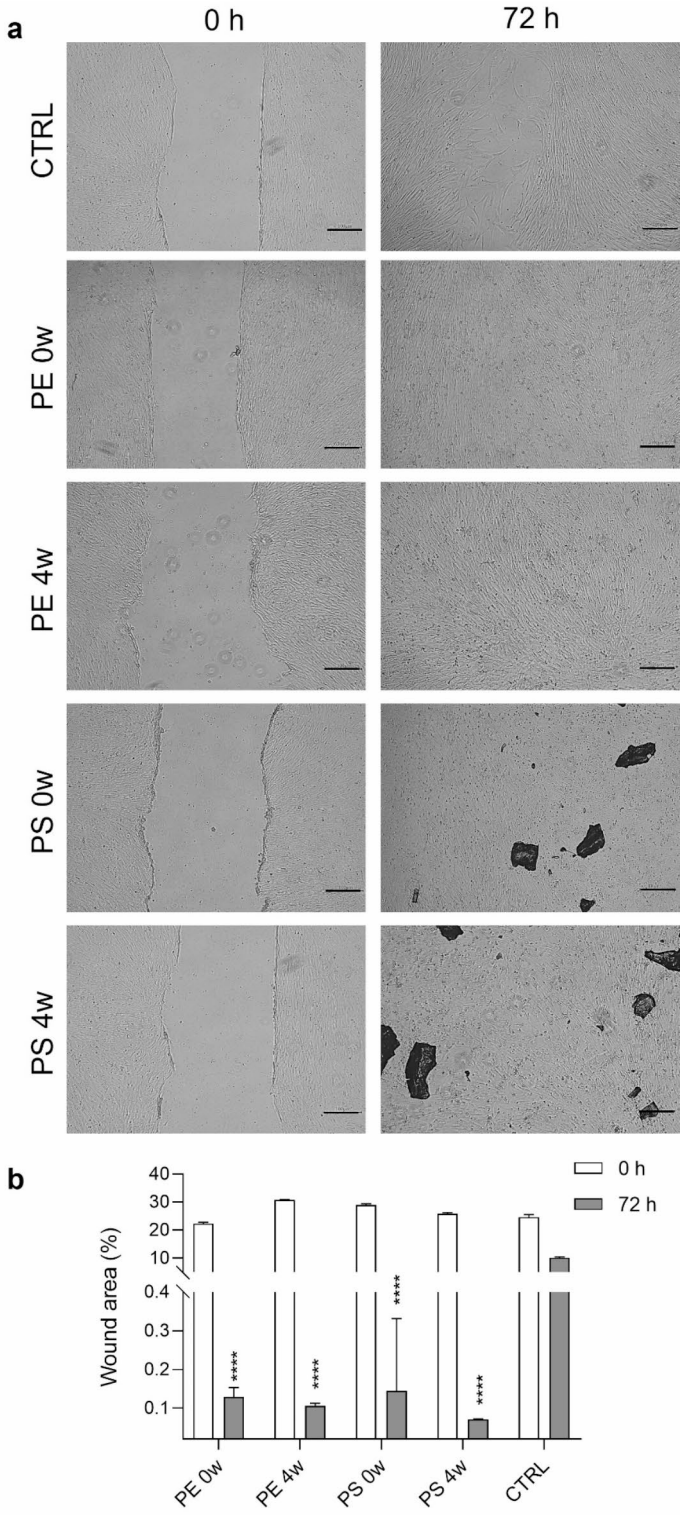

Fig. 3. Migration ability detection in untreated or treated HCASMCs using wound healing assay. a, Micrographs of migration-wound healing assay. Scale bars represent 100 µm. b, Quantification of the gap area as a percentage of the residual area at 0 and 72 h in the same sample. Analysis made using ImageJ software. Data are presented as the means ± SD. Statistical analysis performed using two-way ANOVA followed by Dunnett's post-hoc test. **** $p < 0.0001$ compared to CTRL samples. 0w, virgin MP and 4w, aged materials.

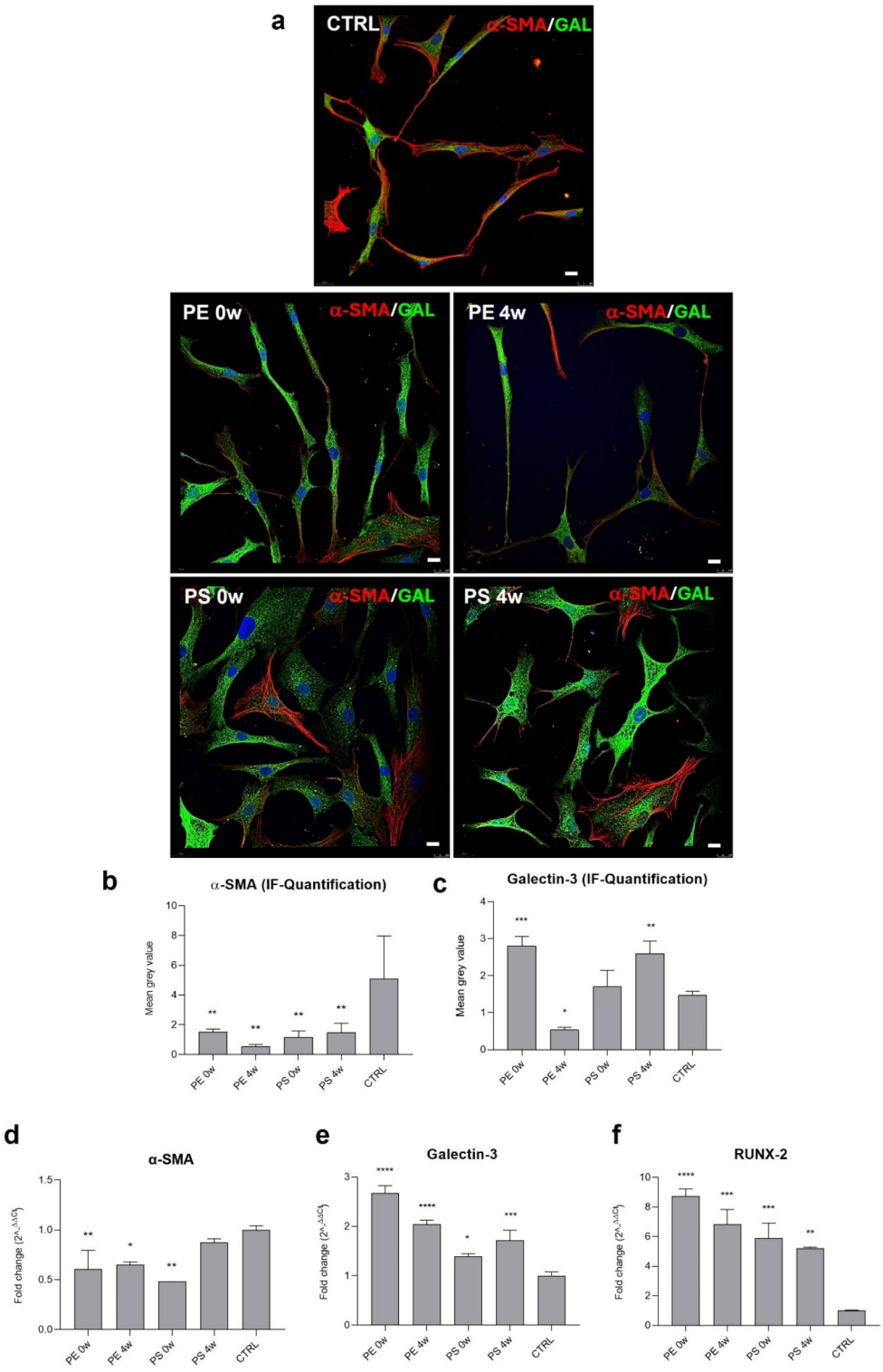

Fig. 4. HCASMCs activation markers evaluation. (a), Confocal representative images of HCASMCS exposed to virgin (0w) and aged (4w) PE and PS for 72 h. Fixed cells were stained for anti-α–smooth muscle actin (α-SMA, in red), anti-galectin-3 (GAL, in green) and DAPI (in blue) to visualise nuclei. Scale bars indicate 10 µm. Immunofluorescence quantification presented as the mean grey value corresponding to (b) α-SMA and (c) galectin-3 in confocal images. Relative expression of (d), α-SMA, (e), galectin-3 and (f), RUNX-2 in HCASMCs treated with virgin and aged PE and PS, either virgin or aged. The expression of each mRNA species was measured by real-time PCR and values were normalised to GAPDH. For Immunofluorescence quantification and RT-CPR, data shown represent the means ± SD. Statistical analysis was made with one-way ANOVA followed by Fisher's LSD post-hoc test. * $p < 0.05$, ** $p < 0.01$, *** $p < 0.001$, **** $p < 0.0001$ compared to CTRL samples.

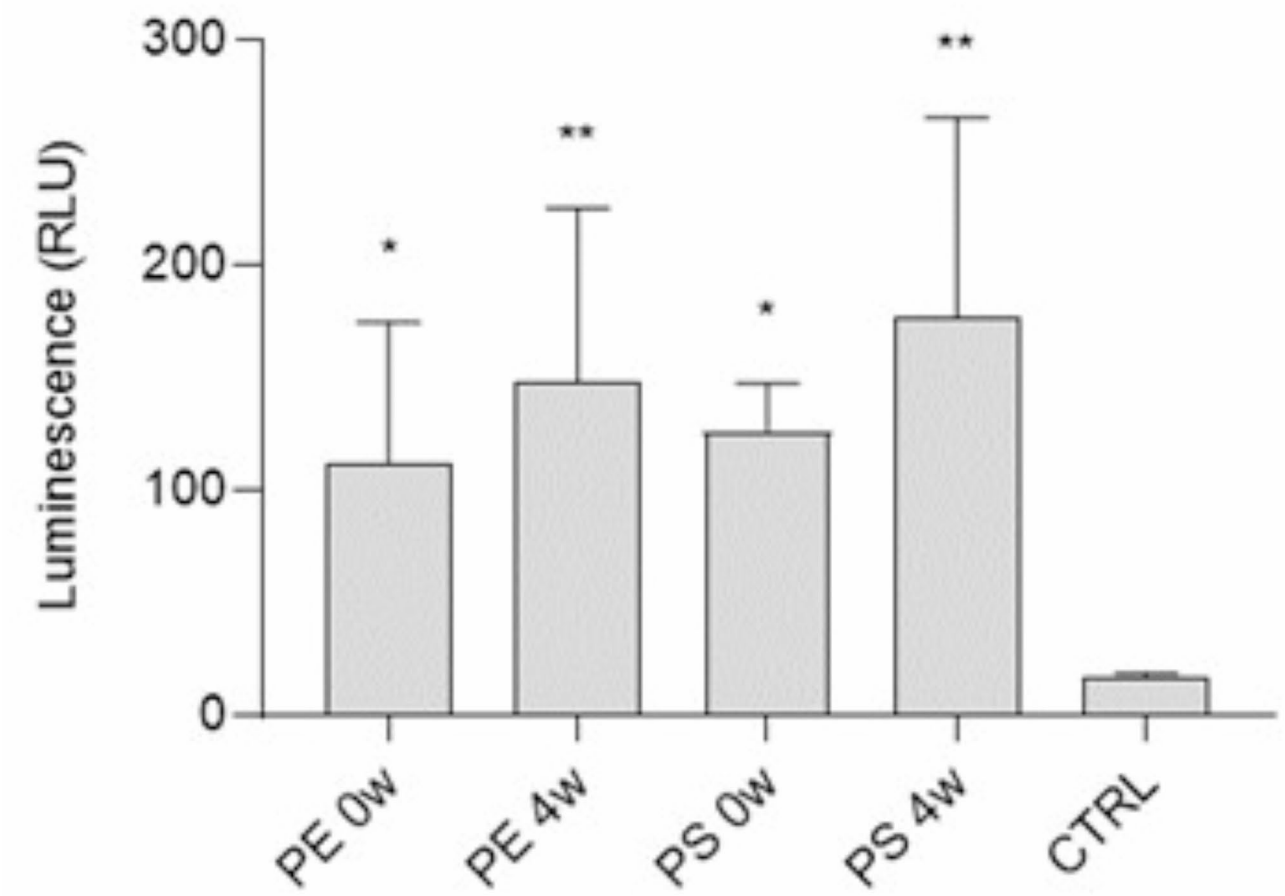

Fig. 5. Caspase-1 induction in control and HCASMC samples treated with different MPs as virgin (0w) or photodegraded materials (4w). Data are shown as the means ± SD. Statistical analysis performed using one-way ANOVA followed by Fisher's LSD post-hoc test. * $p < 0.05$, ** $p < 0.01$ compared to CTRL.

at 72 h compared to control samples. Besides, photodegradation of the plastic fragments further enhanced the activation of caspase-1, which may result in the augmented pro-inflammatory cell phenotype.

Discussion

After entering the organism, MPs can be carried into the bloodstream and distributed throughout the circulatory system to various organs in the body. Studies on mammals proved that nanoparticle exposure to the cardiovascular system impaired cardiac function[1]. The results showed that PS-MPs induced cardiac damage and fibrosis through the Wnt-catenin pathway, collagen production and oxidative stress. Additionally, PS-MPs triggered oxidative stress, apoptosis, and vascular barrier function disruption in human endothelial cells[31]. Altogether, these findings underline that MP exposure may represent an unrecognised risk factor for the development of cardiovascular disease, specifically atherosclerosis. In support of the hypothesis that plastic particles represent emerging health hazards for cardiovascular diseases, recent evidence from a clinical study showed that polyethylene and polyvinyl chloride were found in atheromas from patients undergoing endarterectomy. Furthermore, the presence of MPs (and nanoplastics) in carotid artery plaques reinforced the risk of cardiovascular adverse events, such as myocardial infarction, stroke, or death from any cause among patients[12]. Nonetheless, our current knowledge regarding the precise molecular pathways and cardiotoxicity mechanisms involved in MP exposure remains inadequate.

The present study aims to investigate the role of MPs in promoting vascular smooth muscle cell activation under pathological conditions. The choice of MP-sized material, rather than NP, was dictated by the fact that we did not aim to focus on internalisation but on macromolecular effects and molecular-phenotypic activation of our in vitro model. Corroborating the hypothesis that MP treatment may affect HCASMC homeostasis, the results of the cell viability test showed that these were lower compared to untreated samples (Fig. 1a). These data proved that PE and PS exposure affect the metabolic capacity of HCASMCs as a mirror of cell survival in each sample. Moreover, p53 and BMF were upregulated when both PE and PS were present in the culture media (Fig. 1b and c). p53 is a key transcriptional regulator of apoptosis-related proteins[32]. BMF, a member of the Bcl-2 family, contains only the BH3 domain, which is crucial for inducing apoptosis[33]. The observed results are in line with those from other researchers, reporting how MPs, specifically PS, trigger the apoptosis pathway in mammalian cell models[34,35]. To assess and characterise the potentially toxic and harmful effects of plastic materials, it was

also necessary to screen PE and PS for cytotoxicity in HCASMCs. The LDH detection assay showed an increase in LDH levels in all tested materials (Fig. 2), suggesting cytotoxicity and the destabilisation of the HCASMC cell membrane after MP exposure. Indeed, the reported findings pose the physical basis of vascular cell membrane damage caused by MPs. In support of this, Wang et al.. described not only an augmented LDH production upon PE-nanoparticles exposure but also lipid membrane disruption and variation in the composition and chemical properties[36]. Despite the differences in cell membrane composition, both PE- and PS-MPs were found to cause varying levels of damage to the plasma membrane of *Microcystis aeruginosa*[37].

Contractile VSMCs are the most represented and important cell types in healthy blood vessels. They may alter their proliferation and migration patterns to participate in tissue repair. The phenotypic change from a contractile to a synthetic/activated phenotype includes the activation and expression of specific genes and plays an essential role in the pathophysiology of atherosclerosis. Indeed, in the atherosclerotic lesion, the synthetic phenotype transformation occurs within the walls of blood vessels. Synthetic VSMCs migrate towards the lesion site and secrete cytokines, inflammation factors, chemoattractants, extracellular matrix, and matrix metalloproteinases, which concur with the lesion formation. Implying an increased migration propensity, we then tested HCASMCs undertaking virgin and photodegraded PE and PS treatment. We found that exposure to these treatments indeed increased migration (Fig. 3a and b). For all samples, we noted nearly complete gap closures, meaning an activated migratory propensity.

Additionally, the in vitro expression of galectin-3 was upregulated in all treated samples compared to the control (Fig. 4c and e). Galectin-3 has been recently demonstrated to be a novel inflammatory mediator, participating in intravascular inflammation, lipid endocytosis, macrophage activation, monocyte chemotaxis, and cell adhesion and is involved in the phenotype transformation of VSMCs[23,38]. Similarly, after 72-hour treatment of HCASMCs with either virgin or aged PE and PS, we observed an upregulation in the expression of RUNX-2 (Fig. 4f). This result is significant because RUNX-2 is an important regulator of adverse cellular events that drive cardiovascular pathology. Recent studies have shown that RUNX-2 is a crucial regulator in the osteogenic conversion of arteriosclerotic lesions and strongly correlates with vessel calcification in mouse models[39,40]. These findings were also confirmed in ex vivo human arterial tissue, suggesting that RUNX-2 may have a chemoattractant function on immune system cells, which can then trigger inflammatory responses and thus affect local endothelial and muscle cells[41]. Our evidence uncovered that the MPs tested enhanced RUNX-2 expression, suggesting an activated status that may contribute to the pre-atherosclerotic conversion of HCASMCs. These findings, together with the downregulation in α-SMA (Fig. 4b and d), depict a potential role for MPs in the conversion to a more pathological phenotype. α-SMA expression in the aged PS group did not evidence differences with the control. As the other activation markers were increased, this may be due to the rapid turnover of aged-PS-injured HCASMCs solely, which created a mixed population of cells, also expressing normal markers, such as α-SMA. The migratory phenotype, sustained by the switching to pro-atherogenic genes, was prompted by PE- and PS-MPs exposure and might directly cause extracellular matrix protein secretion and vascular intima infiltration in activated HCASMCs. The activated phenotype described could represent the initial step in atherosclerotic plaque formation, driven by the presence of plastic fragments.

In a recent study, inflammatory biomarkers were found to be elevated in patients' atheromatous plaque, which strongly correlated with the presence of plastic fragments in specimens. Nevertheless, the presence of MPs correlated with cardiovascular events; thus, even if direct casualty could not be proven, these data at least demonstrated a predisposition for cardiovascular risk driven by MPs[12]. To explain the molecular process involved in HCASMC activation following MPs exposure, we measured the inflammasome complex activation. We consistently observed induction of caspase-1 through bioluminescence in all samples exposed to MPs compared to controls (Fig. 5). Caspase-1 activation induces the processing and release of cytokines IL-1β and IL-18, and thus, a coronary artery musculature pro-inflammatory status may be triggered upon PE and PS fragments exposure and cell loss, confirmed by caspase-1 presence. The pro-inflammatory status in HCASMCs potentially contributes to enhanced vascular calcification and atherosclerosis.

In summary, although the precise health consequences of MPs on the human cardiovascular system are still not entirely comprehended, our study demonstrated that MPs could pose various potential health hazards. These risks encompass phenotypic activation, inflammation, and cell damage. Understanding the cellular and molecular mechanisms underlying the toxicity of MPs can identify critical harm pathways and potential intervention and/or prevention targets. It is evident that addressing the issue of MPs pollution requires action, as plastic waste has exponentially increased over the last decades. To better elucidate the health hazard related to the MP samples with the "real" settings, we employed photodegraded MPs, which better mimic the exposure to the in vivo environment. Environmental MPs undergo extensive weathering, and once discarded, they are subjected to the influence of ageing factors present in the environment. Ageing factors are represented by sunlight radiation, seawater flow, and temperature. Recent evidence proved that ageing processes could change the surface structure and chemical composition of MPs and that additives and low-molecular organic products can also be released from aged MPs into the surroundings, potentiating the chemical risk[42]. For these reasons, degraded MP particles were applied to HCASMCs to unveil any potentiation in the detrimental effects of ageing factors acting on MPs, together with the intrinsic effects of the MPs type itself. Our findings indicate a potential cardiovascular risk linked to MPs exposure, and the importance of this study is in identifying PE- and PS-MPs, commonly used in the food industry, as causal factors in the pathological activation of VSMCs. These results partially explain observations from ex vivo human specimens[12], where the presence of MPs has been suggested as a contributing factor to cardiovascular hazards.

Study limitations

Despite some breakthroughs in understanding the cardiovascular risk associated with MPs exposure, this study also has some limitations. First, further investigations are necessary to understand the long-term effects of MPs

exposure entirely. Moreover, although the concentration tested is consistent with doses studied in other works already present in literature[29,43,44], it may not represent the real scenario; a realistic blood concentration should undoubtedly be used. It also remains to be determined how plastic particles are transported to the cardiovascular system, whether they are consistently present in the blood and/or are carried by specific cell types. Also, another question that should be addressed is if MPs can permeate within the blood vessels (i.e., internalised within VSMCs) directly, exerting their toxic effects on the cardiovascular system or indirectly, in terms of substances released by MPs within the bloodstream. Moreover, the MPs used in our study were notably larger (564 μm to 632 μm) than those typically reported in human blood systems and thrombi, which are generally under 100 μm. We acknowledge that smaller MPs are more relevant for human exposure studies, mainly due to their ability to enter the bloodstream and interact with human cells. However, we chose the larger MPs as a preliminary model to investigate the general effects on HCASMCs using virgin and aged materials. To our knowledge, there is limited availability of aged microplastics smaller than 100 μm in existing literature, making our selection a reasonable compromise. Most studies use commercially available polymer particles, particularly PS beads, which do not accurately represent real environmental micro- and nano-plastics (MNPs) due to differences in surface chemistry, particle morphology, and molecular release profiles, with limited real-scenario relevance.

Furthermore, reported particle sizes in studies are an average of the distribution and are therefore conservative, as smaller particles are likely to be present in the environment. Our findings provide a baseline understanding of cellular interactions with MPs. In general, larger particles have a reduced specific surface area compared to smaller particles, leading to fewer interactions with cells and a lower release rate of molecular species. Consequently, the overall impact on cells might be diminished with larger particles. Therefore, the effects observed in our work should be considered a minimum threshold, and our evaluations are conservative compared to the potentially higher effects of smaller particles.

Data availability

The datasets used and/or analyzed during the current study are available from the corresponding author upon reasonable request.

Received: 27 August 2024; Accepted: 3 February 2025
Published online: 04 February 2025

References

1. Persiani, E. et al. Microplastics: A Matter of the Heart (and Vascular System). *Biomedicines* 11, (2023).
2. Emenike, E. C. et al. From oceans to dinner plates: the impact of microplastics on human health. *Heliyon* **9**, e20440 (2023).
3. La Porta, E. et al. Microplastics and kidneys: an update on the evidence for deposition of Plastic Microparticles in Human organs, tissues and fluids and renal toxicity concern. *Int. J. Mol. Sci.* **24**, 14391 (2023).
4. Lomonaco, T. et al. Type-specific inflammatory responses of vascular cells activated by interaction with virgin and aged microplastics. *Ecotoxicol. Environ. Saf.* **282**, 116695 (2024).
5. Yang, Y. et al. Detection of various microplastics in patients undergoing cardiac surgery. *Environ. Sci. Technol.* **57**, 10911–10918 (2023).
6. Fournier, S. B. et al. Nanopolystyrene translocation and fetal deposition after acute lung exposure during late-stage pregnancy. *Part. Fibre Toxicol.* **17**, 55 (2020).
7. Li, Z. et al. Polystyrene microplastics cause cardiac fibrosis by activating Wnt/β-catenin signaling pathway and promoting cardiomyocyte apoptosis in rats. *Environ. Pollut.* **265**, 115025 (2020).
8. Jones, A. E. et al. Inhibition of prostaglandin synthesis during polystyrene microsphere-induced pulmonary embolism in the rat. *Am. J. Physiol. Lung Cell. Mol. Physiol.* **284**, L1072–1081 (2003).
9. Barshtein, G. et al. Polystyrene nanoparticles activate erythrocyte aggregation and adhesion to endothelial cells. *Cell. Biochem. Biophys.* **74**, 19–27 (2016).
10. Wu, D. et al. Pigment microparticles and microplastics found in human thrombi based on Raman spectral evidence. *J. Adv. Res.* **49**, 141–150 (2023).
11. Roshanzadeh, A. et al. Exposure to nanoplastics impairs collective contractility of neonatal cardiomyocytes under electrical synchronization. *Biomaterials* **278**, 121175 (2021).
12. Marfella, R. et al. Microplastics and nanoplastics in Atheromas and Cardiovascular events. *N. Engl. J. Med.* **390**, 900–910 (2024).
13. Cao, G. et al. How vascular smooth muscle cell phenotype switching contributes to vascular disease. *Cell. Commun. Signal.* **20**, 180 (2022).
14. Petsophonsakul, P. et al. Role of vascular smooth muscle cell phenotypic switching and calcification in aortic aneurysm formation. *Arterioscler. Thromb. Vasc Biol.* **39**, 1351–1368 (2019).
15. Tang, H. Y. et al. Vascular smooth muscle cells phenotypic switching in Cardiovascular diseases. *Cells* **11**, 4060 (2022).
16. Zhang, F., Guo, X., Xia, Y. & Mao, L. An update on the phenotypic switching of vascular smooth muscle cells in the pathogenesis of atherosclerosis. *Cell. Mol. Life Sci.* **79**, 6 (2021).
17. Han, M., Wen, J. K., Zheng, B., Cheng, Y. & Zhang, C. Serum deprivation results in redifferentiation of human umbilical vascular smooth muscle cells. *Am. J. Physiol. Cell. Physiol.* **291**, C50–58 (2006).
18. Poliseno, L. et al. Resting smooth muscle cells as a model for studying vascular cell activation. *Tissue Cell.* **38**, 111–120 (2006).
19. Lin, M. E., Chen, T., Leaf, E. M., Speer, M. Y. & Giachelli, C. M. Runx2 expression in smooth muscle cells is required for arterial medial calcification in mice. *Am. J. Pathol.* **185**, 1958–1969 (2015).
20. Chen, Y., Zhao, X. & Wu, H. Transcriptional programming in arteriosclerotic disease: a multifaceted function of the Runx2 (runt-Related transcription factor 2). *Arterioscler. Thromb. Vasc Biol.* **41**, 20–34 (2021).
21. Blanda, V., Bracale, U. M., Di Taranto, M. D. & Fortunato, G. Galectin-3 in Cardiovascular diseases. *Int. J. Mol. Sci.* **21**, 9232 (2020).
22. Tian, L., Wang, Y. & Zhang, R. Galectin-3 induces vascular smooth muscle cells calcification via AMPK/TXNIP pathway. *Aging (Albany NY).* **14**, 5086–5096 (2022).
23. Papaspyridonos, M. et al. Galectin-3 is an amplifier of inflammation in atherosclerotic plaque progression through macrophage activation and monocyte chemoattraction. *Arterioscler. Thromb. Vasc Biol.* **28**, 433–440 (2008).
24. Prata, J. C. et al. Solutions and Integrated strategies for the Control and Mitigation of Plastic and Microplastic Pollution. *Int. J. Environ. Res. Public. Health.* **16**, 2411 (2019).
25. Zuccarello, P. et al. Exposure to microplastics (<10 μm) associated to plastic bottles mineral water consumption: the first quantitative study. *Water Res.* **157**, 365–371 (2019).

26. Biale, G. et al. A systematic study on the Degradation products generated from artificially aged Microplastics. *Polym. (Basel)*. **13**, 1997 (2021).
27. Lomonaco, T. et al. Release of harmful volatile organic compounds (VOCs) from photo-degraded plastic debris: a neglected source of environmental pollution. *J. Hazard. Mater.* **394**, 122596 (2020).
28. Castelvetro, V. et al. New methodologies for the detection, identification, and quantification of microplastics and their environmental degradation by-products. *Environ. Sci. Pollut Res.* **28**, 46764–46780 (2021).
29. Wang, Y. L. et al. The kidney-related effects of Polystyrene Microplastics on human kidney proximal tubular epithelial cells HK-2 and male C57BL/6 mice. *Environ. Health Perspect.* **129**, 57003 (2021).
30. Persiani, E., Ceccherini, E., Gisone, I., Cecchettini, A. & Vozzi, F. Protocol to generate an in vitro model to study vascular calcification using human endothelial and smooth muscle cells. *STAR. Protoc.* **4**, 102328 (2023).
31. Chen, Y. C. et al. Evaluation of toxicity of polystyrene microplastics under realistic exposure levels in human vascular endothelial EA.hy926 cells. *Chemosphere* **313**, 137582 (2023).
32. Aubrey, B. J., Kelly, G. L., Janic, A., Herold, M. J. & Strasser, A. How does p53 induce apoptosis and how does this relate to p53-mediated tumour suppression? *Cell. Death Differ.* **25**, 104–113 (2018).
33. Puthalakath, H. et al. Bmf: a proapoptotic BH3-only protein regulated by interaction with the myosin V actin motor complex, activated by anoikis. *Science* **293**, 1829–1832 (2001).
34. An, R. et al. Polystyrene microplastics cause granulosa cells apoptosis and fibrosis in ovary through oxidative stress in rats. *Toxicology* **449**, 152665 (2021).
35. Wang, X., Zhang, X., Sun, K., Wang, S. & Gong, D. Polystyrene microplastics induce apoptosis and necroptosis in swine testis cells via ROS/MAPK/HIF1α pathway. *Environ. Toxicol.* **37**, 2483–2492 (2022).
36. Wang, W. et al. Effects of polyethylene microplastics on cell membranes: a combined study of experiments and molecular dynamics simulations. *J. Hazard. Mater.* **429**, 128323 (2022).
37. Zheng, X. et al. Growth inhibition, toxin production and oxidative stress caused by three microplastics in Microcystis aeruginosa. *Ecotoxicol. Environ. Saf.* **208**, 111575 (2021).
38. Tian, L. et al. Galectin–3 induces the phenotype transformation of human vascular smooth muscle cells via the canonical wnt signaling. *Mol. Med. Rep.* **15**, 3840–3846 (2017).
39. Tanaka, T. et al. Runx2 represses myocardin-mediated differentiation and facilitates osteogenic conversion of vascular smooth muscle cells. *Mol. Cell. Biol.* **28**, 1147–1160 (2008).
40. Al-Huseini, I., Ashida, N. & Kimura, T. Deletion of IκB-Kinase β in smooth muscle cells induces vascular calcification through β-Catenin-runt-related transcription factor 2 signaling. *J. Am. Heart Assoc.* **7**, e007405 (2018).
41. Ukkat, J., Hoang-Vu, C., Trojanowicz, B. & Rebelo, A. Osteocalcin, osteopontin and RUNX2 expression in patients' leucocytes with arteriosclerosis. *Diseases* **9**, 19 (2021).
42. Liu, P. et al. Review of the artificially-accelerated aging technology and ecological risk of microplastics. *Sci. Total Environ.* **768**, 144969 (2021).
43. Brown, D. M., Wilson, M. R., MacNee, W., Stone, V. & Donaldson, K. Size-dependent proinflammatory effects of ultrafine polystyrene particles: a role for surface area and oxidative stress in the enhanced activity of ultrafines. *Toxicol. Appl. Pharmacol.* **175**, 191–199 (2001).
44. Deng, Y., Zhang, Y., Lemos, B. & Ren, H. Tissue accumulation of microplastics in mice and biomarker responses suggest widespread health risks of exposure. *Sci. Rep.* **7**, 46687 (2017).

Acknowledgements

The authors would like to thank Laura Poliseno and her research group, in particular Antonella Prantera, and Lorena Tedeschi, as well as Silvia Del Ry and Manuela Cabiati, all based at CNR, Institute of Clinical Physiology, for their technical support in performing the qPCR analysis.

Author contributions

Conceptualisation: Elisa Persiani, Antonella Cecchettini, Federico Vozzi; Investigation: Elisa Persiani, Sofia Amato, Antonella Cecchettini; Writing-original draft: Elisa Persiani, Antonella Cecchettini; Writing-review and editing: Elisa Persiani, Antonella Cecchettini, Elisa Ceccherini, Ilaria Gisone, Sofia Amato, Agnese Sgalippa, Chiara Ippolito, Valter Castelvetro, Tommaso Lomonaco, Federico Vozzi; Supervision: Federico Vozzi. All authors have read and agreed to the published version of the manuscript.

Funding

No funding was received to assist with the preparation of this manuscript.

Declarations

Competing interests

The authors declare no competing interests.

Additional information

Supplementary Information The online version contains supplementary material available at https://doi.org/10.1038/s41598-025-89006-z.

Correspondence and requests for materials should be addressed to F.V.